Arabian Journal of Chemistry (2020) 13, 9130–9138

King Saud University

Arabian Journal of Chemistry

www.ksu.edu.sa
www.sciencedirect.com

ORIGINAL ARTICLE

Influence of impregnation conditions on the activity of CrO_x/Al_2O_3 catalysts in dehydrogenation of isobutane in fixed bed reactor

A.I. Zolotukhina [a], E.V. Romanova [a], T.A. Bugrova [a], A.S. Knyazev [a,b], G.V. Mamontov [a,*]

[a] Tomsk State University, Tomsk, Russia
[b] LLC 'Engineering Chemical Technological Center', Tomsk, Russia

Received 13 August 2020; accepted 26 October 2020
Available online 4 November 2020

KEYWORDS

CrO_x/Al_2O_3 catalysts;
Vacuum impregnation;
Isobutane dehydrogenation;
Fixed bed reactor;
Catalyst granules, Hierarchical structure

Abstract The development of catalysts for dehydrogenation of light paraffin hydrocarbons in a fixed bed reactor is of great importance for the world petrochemical industry. The preparation of granules (~3 mm in diameter) of CrO_x/Al_2O_3 catalysts is hindered by such problems as homogeneous distribution of active component and modifiers, high strength of granules, etc. In this paper, the alumina support dissolution in the impregnating solution containing chromic acid and the opportunity to apply vacuum impregnation to minimize this effect in the preparation of CrO_x/Al_2O_3 catalysts are discussed. A series of catalysts is synthesized at different impregnation pressures (1, 0.85, and 0.7 atm), characterized by a complex of physical–chemical methods (low-temperature N_2 adsorption, SEM, XRD, TPR-H_2), and tested in isobutane dehydrogenation. The use of vacuum impregnation is shown to lead to the reduction of the specific surface area of the catalysts from to 91 to 56 m^2/g and the growth of content of CrO_x phases that decreases the catalytic activity in dehydrogenation. The isobutylene yield at 610 °C decreases from 68% to 54% for the catalyst prepared at P = 0.7 atm as compared with the one prepared at atmospheric pressure. The high activity and stability are connected with the hierarchical structure of the alumina support and homogeneous chromia distribution on its surface.

1. Introduction

At present, the demand in olefin hydrocarbons steadily grows due to the rising production of polymers and chemical compounds on the basis thereof. Thermal and catalytic cracking of heavy hydrocarbons (mainly oil) and dehydrogenation of paraffins are the major industrial methods to manufacture the unsaturated hydrocarbons. The processes of catalytic

* Corresponding author.
E-mail address: GrigoriyMamontov@mail.ru (G.V. Mamontov).
Peer review under responsibility of King Saud University.

ELSEVIER Production and hosting by Elsevier

https://doi.org/10.1016/j.arabjc.2020.10.037
1878-5352

dehydrogenation of hydrocarbons (STAR, Oleflex, BASF-Linde process, Catofin, FDB by Snamprogetti and Yarsintez) are among the priority processes in the petrochemical industry (Sattler et al., 2014), with the dehydrogenation of light paraffins with the oxidants (oxygen or carbon dioxide) over various catalysts being widely discussed in the literature (Fattahi et al., 2013, 2011; Darvishi et al., 2016; Bugrova et al., 2019).

Various catalysts have been proposed for the dehydrogenation of light paraffins, including conventional catalysts based on deposited precious metals, primarily platinum (Long et al., 2014; Li et al., 2017; Zhou et al., 2017), chromium (Słoczyński et al., 2011; Li et al., 2016; Cheng et al., 2015), and vanadium (Rodemerck et al., 2016, 2017; Tian et al., 2016) oxides, and also the catalysts based on ordered mesoporous materials (Xu et al., 2013; Shee and Sayari, 2010), metal–organic frameworks (Zhao et al., 2013), activated carbon (Xu et al., 2014; Li et al., 2015), zirconia (Otroshchenko et al., 2015, 2016) and even bare alumina (Rodemerck et al., 2016). The γ-Al_2O_3-supported chromium oxide catalysts are widely used in industry (Ruettinger et al., 2010; Busygin et al., 2013) in the processes with fluidized bed of microspherical catalysts (Kataev et al., 2015; Gilmanov et al., 2015) and with fixed bed of palletized catalysts (Catofin). According to the patent (Fridman, 2012), the isobutane conversion of ~56% with the selectivity towards isobutylene of 92% may by achieved at ~540 °C when fresh CrO_x/Al_2O_3 catalyst is used. The aged catalyst is characterized by the isobutane conversion of 48% and selectivity of 87.6% at ~565 °C.

There are a number of drawbacks of fluidized-bed paraffin dehydrogenation process such as high toxicity of microspherical Cr-containing catalysts, equipment deterioration, high catalyst consumptionn, and relatively low alkene yields. Thus, the global tendency is connected with the dehydrogenation of paraffins in the fixed-bed reactor or reactors with the moving bed of catalyst as more effective and eco-friendly processes. The synthesis of such catalysts is complicated by the need to prepare the catalyst granules with high porosity, strength and homogeneous distribution of supported active components.

Impregnation technique is mostly used to synthesize the supported catalysts due to simplicity and effectiveness. The γ-Al_2O_3 support granules with diameter of ~3 mm (1/8″) are impregnated with an aqueous solution containing the precursors of the active component and modifiers to prepare the CrO_x/Al_2O_3 catalyst (Fridman, 2012; Ruettinger and Jacubinas, 2016; Salaeva et al., 2020). The CrO_3 is used as a precursor of the active component in industry because of its high solubility (it allows introducing up to ~28 %wt. of Cr_2O_3 into the alumina support), the minimal amount of aggressive gases released during the catalyst calcination as well as the adsorption of chromate ions on the surface of γ-Al_2O_3 leading to the uniform distribution of the active component and its stabilization in a highly dispersed state (Spanos et al., 1994). The main disadvantage of CrO_3 application is low pH of the impregnation solution (pH ≈ 0) because of high concentration of H_2CrO_4 therein that requires the use of special acid-resistant equipment. Aluminum oxide is also known to be dissolved in acids that implies additional requirements to the impregnation conditions.

One of the approaches that makes it possible to shorten the contact time of the impregnation solution with the alumina support is the vacuum impregnation-drying method used in particular to produce microspherical CrO_x/Al_2O_3 catalysts (Bekmukhamedov et al., 2016). The reduced pressure inside the pores of alumina support provides penetration of the impregnating solution in small pores that leads to more homogeneous distribution of the active components in catalyst granules. The impregnation under moderate vacuum may be taken into account for catalyst preparation, since it can be implemented in industry.

The aim of this work was to reveal the influence of impregnation conditions (pressure during impregnation) of a molded alumina support on the properties of the produced alumina catalysts and their activity in the dehydrogenation of paraffin hydrocarbons with a fixed bed catalyst. A series of catalysts were synthesized with different pressures during the impregnation, studied by a complex of physical–chemical methods, and tested in the fixed-bed isobutane dehydrogenation.

2. Experimental part

The alumina support was prepared using a thermochemically activated aluminum trihydroxide (TCA THA) that was extruded with a small amount of nitric acid and 2 wt% of wood flour as a porogen (Bugrova et al., 2016) into cylindrical granules with a diameter of ~3 mm and a length of 4–6 mm. The support granules were dried at 120 °C and calcined at 700 °C for 4 h. The temperatures of drying and calcination were previously optimized taking into account the phase transformation of alumina hydroxides and boehmite into γ-Al_2O_3 without the transformation into δ- or α-Al_2O_3 with lower specific surface area (Zykova et al., 2015). The conditions were close to those used to prepare the industrial CrO_x/Al_2O_3 catalysts (Fridman, 2012).

To study the stability of the alumina support towards impregnating solution, a model impregnating solution with pH≈0 containing 2.29 %wt. of chromium and 0.35 %wt. of potassium were prepared by dissolving the corresponding amounts of CrO_3 (chemically pure, Vekton, Russia) and KNO_3 (chemically pure, Vekton, Russia). The support granules were placed into the model impregnation solution, then the probe of solution (~100 μl) was taken every 5–7 min to determine the content of Cr, K, and Al by atomic emission spectroscopy (“Agilent 4100″ spectrometer with microwave plasma).

Chromia-containing catalysts were prepared by impregnation using an aqueous solution of precursors of the active component (CrO_3, chemically pure) and alkaline modifier (KNO_3, chemically pure). The excess of impregnating solution (15.2 ml) was prepared by dissolution of CrO_3 (10.3 g) and KNO_3 (1.7 g) in distilled water. The loadings of the components in the catalyst were 20 %wt. Cr_2O_3 and 2 %wt. K_2O, which was close to those in industrial catalysts (Li et al., 2015; Otroshchenko et al., 2016; Fridman and Urbancic, 2015). The alumina support granules were dried at 150 °C overnight to remove the moisture. Then the granules (10 g) were put into the three-neck flask equipped with the vacuum pump and dropping funnel with a pressure compensator. The support granules were degassed at 1.0, 0.85 and 0.70 atm for 20 min, then the excess of the impregnating solution was added from the dropping funnel at pressures of 1.0, 0.85, and 0.7 atm. After that, the flask was opened accurately, and the pressure was normalized to the atmospheric one. The

excess of impregnating solution was drained. The impregnated granules were immediately dried at 95 °C and calcined at 400 °C for 2 h.

Chemical analysis of the samples was carried out by dissolving them in a mixture of sulfuric and nitric acids and analyzing the resulting solution by atomic emission spectroscopy (AES) using the "Agilent 4100″ spectrometer with microwave plasma. The porous structure of the samples was carried out by low-temperature (77 K) nitrogen adsorption using the "Tristar 3020″ analyzer (Micromeritics, USA). The determination of the specific surface area (S_{BET}) was carried out using the multipoint BET method to straighten the nitrogen adsorption isotherm in the range of relative pressures p/p_o from 0.05 to 0.30. The pore size distribution was obtained using the BJH-desorption method analyzing the desorption branch of nitrogen adsorption–desorption isotherm. The Hg intrusion porosimetry measurements were carried out using the Poremaster-33 (Quantachrome, USA).

The phase composition of the synthesized catalysts was studied by powder X-ray diffraction (XRD) using the Shimadzu XRD 6000 diffractometer with CuKα radiation and a Ni-filter. The diffraction peaks of the crystalline phases were processed using the POWDER CELL 2.4 software and compared with those peaks of standard compounds from the PCPDFWIN database. The sizes of the crystallites of the metal oxides were calculated using the Scherrer equation. The scanning electron microscopy (SEM) was used to characterize the broken granules. The SEM 515 (Philips) microscope with the accelerating voltage of 30 kV was used. The features of the sample reduction were studied by the temperature-programmed reduction (TPR-H_2). The experiments were carried out on the chemisorption analyzer ChemiSorb 2750 (Micromeritics, USA) for as-prepared samples using a 10% H_2/Ar gas mixture at a flow rate of 20 ml/min and a heating rate of 10 deg/min.

Catalytic properties of the samples were studied through the isobutane dehydrogenation. The experiments were carried out on the "Katakon" flow catalytic unit (Katakon, Russia) in a tubular metal reactor with a stationary catalyst bed at temperatures of 570, 590, 610 °C. A reaction mixture of 15% i-C_4H_{10} and the balance of Ar was fed through a catalyst bed (10 cm^3 of catalyst pellets, 8.5–9.0 g) at a rate of 25.2 l/h. The experiment was carried out in a cyclic mode: reduction (H_2/Ar mixture, 3 min), dehydrogenation (isobutene, 9 min), regeneration (atmosphere-air, 9 min). The Ar flow (3 min) was fed through the catalysts between each step. The gas probe for analysis was taken at 7th min of the dehydrogenation step. Analysis of the reaction mixture and reaction products was carried out using the gas chromatograph "Khromos GKh-1000" (Khromos, Russia) with a flame ionization detector and two microcatharometers. The products were separated at 50 °C using the quartz capillary column with poly(trimethylsilyl)propene (PTMSP), a packed column with Chromosorb 106 (60/80 mesh) and a packed column with NaX molecular sieves (45/60 mesh). The quantitative calculation of the volume fraction of the components of the gas mixture was determined using the Khromos software 2.16.43. Before the catalytic test, the experiment with quartz balls was carried out. The isobutane conversion was 3–5% at 570–610 °C that indicates the negligible insignificant influence of the inert balls, reactor walls and homogeneous reaction on the catalytic results.

3. Results and discussion

3.1. Study of the stability of alumina granules to solution of chromia precursor

To study the stability of the alumina support in contact with the impregnating solution, the support granules (particles with sizes of 0.5–1 mm) were placed in a model impregnating solution containing 2.35 %wt. of chromium (as CrO_4^{2-} ions) and 0.35 %wt. of potassium (as K^+ ions) with pH ≈ 0. Fig. 1a shows the concentration dependences for chromium, potassium and aluminum in the solution as a function of contact time of alumina granules with the solution. The Cr concentration in the solution drops sharply during the first five minutes of impregnation from 2.29 %wt. to ~1.7 %wt. indicating the sorption of negatively charged chromate ions (CrO_4^{2-}) on the alumina support surface positively charged at pH ~ 0. During the next 40 min, the Cr concentration in the solution changes insignificantly indicating the achievement of the adsorption–desorption equilibrium. The K concentration in the impregnating solution does not change indicating the absence of adsorption of positively charged potassium ions on the positively charged alumina surface.

It is noteworthy that the Al concentration in the model impregnating solution grows rapidly enough indicating the dissolution of alumina support in acidic conditions under the action of a chemically aggressive impregnating solution. At 50 min of granule contact with the solution, the Al concentration in the solution increases up to 0.274 %wt., which corresponds to ~0.8 % support dissolution. The support dissolution in the impregnating solution is a negative effect leading to the formation of mixed chromium-aluminum oxides inactive in the dehydrogenation reaction (Nemykina et al., 2010), decreased specific surface area (Bugrova and Mamontov, 2016), etc. The aluminum presence in excess of the impregnating solution limits the reuse of the latter for impregnating the next support batch under industrial conditions (Mamontov et al., 2017).

Thus, the contact of the impregnating solution containing chromic acid with the alumina support granules was shown to lead to rather rapid alumina dissolution. Reducing of impregnation time is essential to minimize this negative effect. On the other hand, time of alumina granule impregnation should be enough for the impregnating solution to penetrate inside the granules providing homogeneous distribution of active component and alkali modifier. Fig. 1b shows the intact and broken granules of alumina-chromia catalysts prepared by impregnation at atmospheric pressure during 5 and 15 min. The gradient of color from dark-green to yellow and white across the breaks of granules ("egg-shell" structure) is observed after 5 min of alumina support contact with the impregnating solution. This means that 5 min is not enough for homogeneous distribution of active component in the catalyst granules. Impregnation of alumina support during 15 min leads to more homogeneous distribution of active component across the granule diameter (absence of color gradient at the granule break, "whole-egg" structure). Thus, the impregnation time should be optimized to achieve both introduction of active component and minimize the support dissolving. The granule impregnation at reduced pressure may be used to increase the solution penetration rate inside the sup-

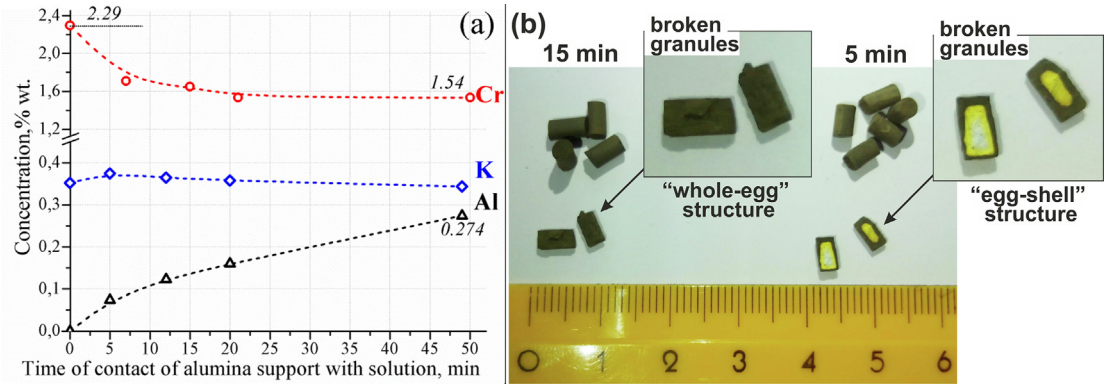

Fig. 1 Concentration dependences for chromium, potassium and aluminum in the model impregnating solution on the contact time of alumina support with solution (a) and photos of alumina-chromia catalysts prepared by impregnation at 1 atm during 5 and 15 min (b).

port pores and minimize the contact time with the solution. This technique may be implemented in industry only in the case of insignificant pressure reduction to 0.5–0.7 atm (Ertl et al., 2008).

3.2. Pressure effect during the impregnation on the activity of alumina-chromia catalysts

Three alumina-chromia catalysts were prepared by varying the pressure during the impregnation (1, 0.85 and 0.7 atm). Table 1 shows the chemical analysis data and textural characteristics of the prepared catalysts. The contents of potassium and chromium oxides in all catalysts are close to the given values (2 %wt. and 20 %wt., respectively). The observed overestimation of the chromium oxide content by about 1%wt. (the nominal loading of 20 wt%) may be a consequence of the Cr precursor sorption on the support during the impregnation from the excess of the impregnating solution. The Cr sorption is observed during the alumina support contact with the model impregnating solution (Fig. 1a). Thus, from the data obtained, it can be concluded that the pressure change during the impregnation does not significantly influence on the catalyst chemical composition.

Fig. 2 shows the SEM images of the catalyst granules (broken immediately before the SEM studies). It can be seen from the SEM images that catalyst structure feature roughness that results from the packing of alumina powder particles during the extrusion. Wide pores with sizes of 10–50 μm and pores with size of from few hundreds nm to few micrometers are observed.

The presence of these pores is important for both the penetration of the impregnating solution during the catalyst preparation and for effective reagent transport during the high temperature catalytic process. The size of primary alumina particles constituting the catalyst structure ranges from several micrometers to ~20 μm (Fig. 2b). The space between these primary particles provides high volume of macropores, and some of them cannot be detected by the SEM.

Fig. 3 shows the N_2 adsorption–desorption isotherms and pore size distributions for alumina support and the catalysts on the basis thereof. The support is characterized by a mesoporous structure that is evidenced by the presence of a hysteresis loop in the region of relative pressures of 0.5–1.0 on the N_2 adsorption–desorption isotherms. The pore size distribution resides in the region from 2 to 20 nm with the distribution maximum at ~5 nm. The support specific surface area and the pore volume are 139 m^2/g and 0.350 cm^3/g, respectively (Table 1). The strength of alumina support granules is calculated as P = F/D*h, where F is a force of granule breaking, D is a granule diameter, and h is a granule length. The measurement for 30 granules show the strength of 8.7 ± 0.5 MPa that is sufficient for industrial catalysts. Thus, the presence of macropores shown by SEM does not decrease the granule strength.

The catalysts are characterized by the decreased specific surface area (56–91 m^2/g) and pore volume (0.166–0.225 cm^3/g). It is clearly seen from Table 1 and Fig. 3a that the pressure decreasing during the impregnation leads to consistently reduced pore volume and specific surface area without significant changes of chemical composition (Table 1). A

Table 1 Textural characteristics and chemical composition of alumina support and catalysts.

Sample	Impregnation pressure, atm	S_{BET}, m^2/g	V_{pore}, cm^3/g	Content of component, % wt.			
				Al_2O_3	K_2O	Cr_2O_3	Σ
Al_2O_3	–	139	0.350	98.88	–	–	98.88
CrO_x/Al_2O_3-1	1.0	91	0.225	75.47	1.83	20.89	98.19
CrO_x/Al_2O_3-0.85	0.85	74	0.184	77.13	2.04	21.15	100.32
CrO_x/Al_2O_3-0.7	0.7	56	0.166	76.93	1.92	21.04	99.89

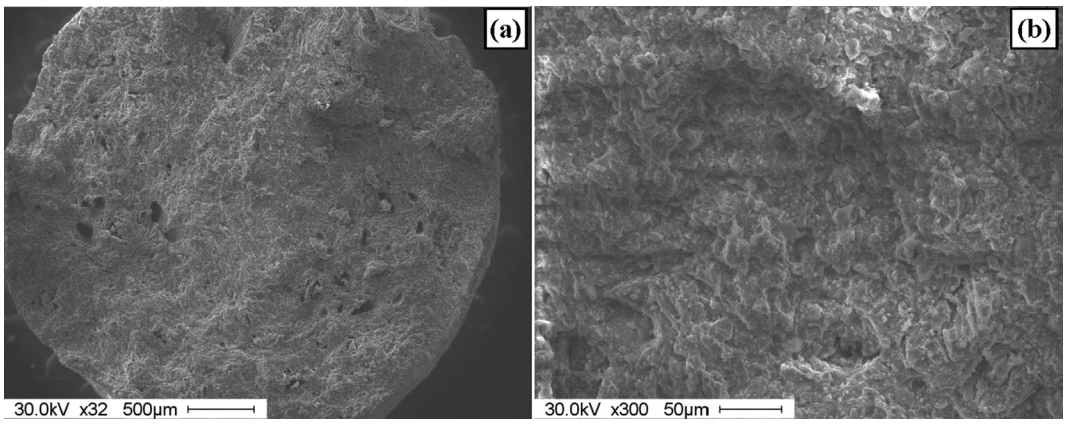

Fig. 2 The SEM images of break of catalyst granules prepared at P = 1 atm.

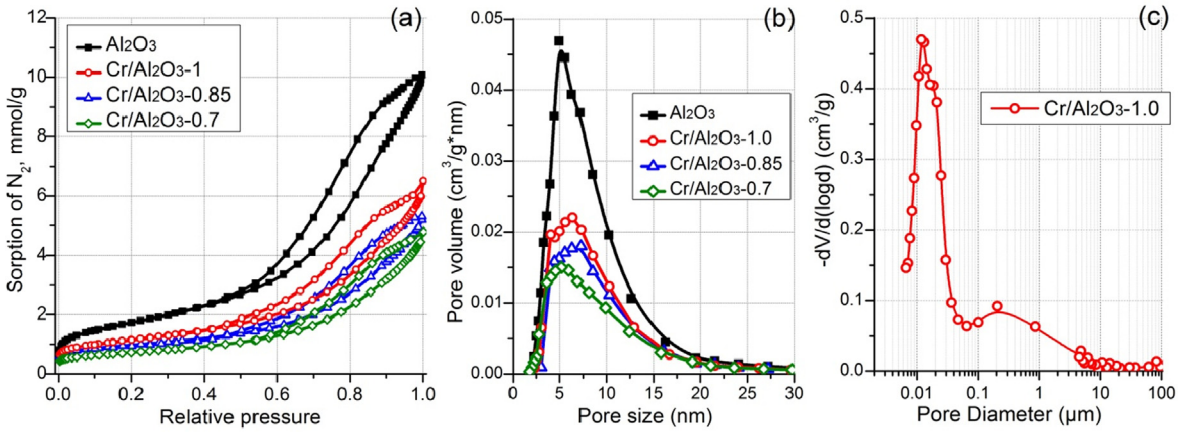

Fig. 3 Nitrogen adsorption–desorption isotherms (a) and pore size distributions (b) for alumina support and prepared catalysts, pore size distribution for Cr/Al_2O_3-1.0 catalyst according to Hg intrusion porosimetry (c).

decreased pore volume throughout the pore size range for the catalysts (Fig. 3b) indicates the active component distribution in the support pores. The shifting of the pore size distribution maximum for Cr/Al_2O_3-0.7 catalyst towards smaller sizes can be caused by coarsening of the CrO_x particles in mesopores with sizes of 5–20 nm. The pore size distribution in the range of 2–3.5 nm for all samples is practically the same, which may indicate the difficulties in the active component penetration into the fine support pores, even if vacuum impregnation is used.

To study the porosity, the Hg intrusion porosimetry was applied for Cr/Al_2O_3-1.0 catalyst. The differential pore size distribution (Fig. 3c) features two types of pores, namely, mesopores with diameter from few nm to ~40 nm and wide macropores with sizes of from 50 nm to ~8 μm with a maximum at ~200 nm. The presence of macropores may be caused by using the wood flour as a porogen during the granule extrusion. These results are consistent with the SEM data. Thus, the catalyst granules are characterized by the hierarchical porous structure (meso- and macropores).

The XRD patterns for the catalysts and the results of qualitative and quantitative analysis of XRD are shown in Fig. 4 and Table 2, respectively. All catalysts feature high content of amorphous phase (68.1–71.5%). The support constitutes

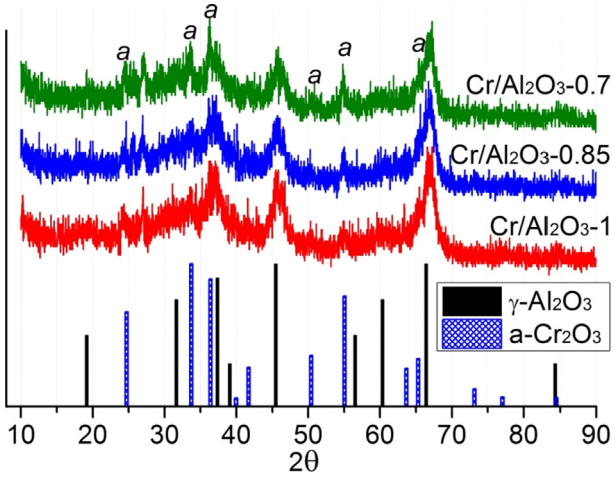

Fig. 4 Powder XRD patterns for prepared catalysts.

the γ-Al_2O_3 and amorphous phases. The active component (CrO_x) exists in the amorphous state, with a small part comprising α-Cr_2O_3 phase. The content of the α-Cr_2O_3 phase increases from 3.4 %wt. to 5.3 %wt. with a pressure decrease during the impregnation from 1.0 to 0.7 atm. The α-Cr_2O_3 par-

Table 2 XRD data for synthesized catalysts.

Catalyst	Phases	The phase content,% wt.	Particle size, nm
CrO_x/Al_2O_3-1	γ-Al_2O_3	25.1	7.0
	α-Cr_2O_3	3.4	7.0
	Amorphous phase	71.5	–
CrO_x/Al_2O_3-0.85	γ-Al_2O_3	24.7	7.1
	α-Cr_2O_3	4.2	15.3
	Amorphous phase	71.1	–
CrO_x/Al_2O_3-0.7	γ-Al_2O_3	26.6	6.7
	α-Cr_2O_3	5.3	20.4
	Amorphous phase	68.1	–

ticle size (coherent scattering region) increases from 7.0 to 15.3 and 20.4 nm for pressure of impregnation of 1.0, 0.85 and 0.7 atm, respectively. This may explain the decreased specific surface area of the catalysts obtained under reduced pressure due to the partial blocking of the alumina support pores by chromia particles.

Fig. 5 shows the TPR results for the obtained samples. All catalysts are characterized by the hydrogen consumption in the temperature range from 200 °C to 450 °C associated with the Cr(VI) reduction to Cr(III) (Bugrova et al., 2019). Two peaks of hydrogen consumption are observed for Cr/Al_2O_3-1 catalyst indicating coexistence of two Cr(VI) states. The first peak with a maximum at 320 °C can be attributed to the reduction of monomeric and/or oligomeric forms of Cr (VI) (Fridman et al., 2016). In our previous work (Salaeva et al., 2020), using Raman spectroscopy, we showed the key roles of monomeric and dimeric chromia species in isobutane dehydrogenation. A high-temperature peak at 420 °C may be attributed to reduction of small particles of Cr (VI) oxide or potassium chromates (Neri et al., 2004; Rombi et al., 2003). The shifting of TPR peak from 320 °C to 360 °C may be caused by an increase in the particle size of the chromium (VI) compounds or increased interaction of chromia species with alumina, which both lead to the decreasing of the catalytic activity (Salaeva et al., 2019).

Thus, from the TPR results it can be concluded that aside from α-Cr_2O_3 detected by XRD, the catalysts contain the Cr (VI) species that are reduced at 200–450 °C. The reductive pre-

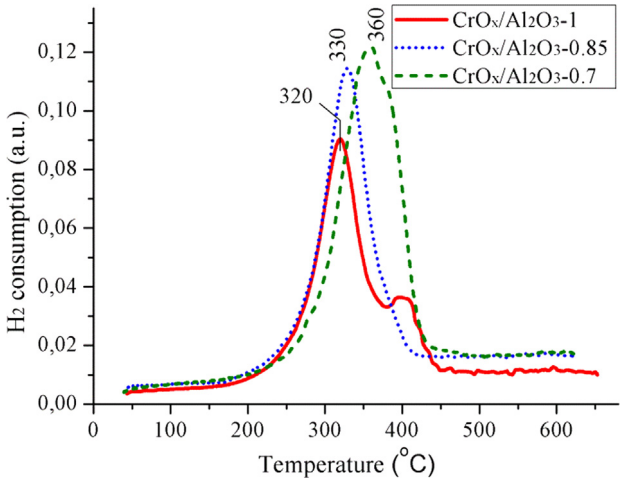

Fig. 5 TPR H_2 profiles for prepared catalysts.

treatment of the catalysts before the catalytic experiments leads to Cr(VI) reduction into Cr(III) sites (Bugrova and Mamontov, 2018). The real state of the active catalyst surfaces during the dehydrogenation is presented by two types of Cr (III) species: the first one is Cr(III) found in the as-prepared catalysts (including α-Cr_2O_3 detected by XRD) and Cr(III) formed due to the Cr(VI) species reduction. The activity of these species depends on both their dispersion and distribution on the catalysts surface. According to N_2 physisorption and TPR results, the chromia species distribution is more homogeneous for the catalyst prepared at atmospheric pressure. Thus, the use of vacuum impregnation allows obtaining the catalysts with high content of Cr(VI) species, but with the decreased dispersion of these species. Consequently, the decreased Cr(VI) dispersion may be the reason for reduced catalytic activity.

The catalytic properties of the prepared catalysts were studied in isobutane dehydrogenation in a fixed-bed reactor (Fig. 6). The real catalyst granules were tested under conditions close to the industrial ones to show the real opportunity for catalyst application in the process. The isobutane conversion growth is observed for all catalyst as the temperature increases from 570 °C to 610 °C with the corresponding decreasing of isobutylene selectivity. The conversion growth in this temperature region indicates the minimal diffusion limitations that are attributed to the presence of macropores in the catalyst granules shown by the SEM. The catalyst synthesized by the impregnation at atmospheric pressure is characterized by higher catalytic activity. Thus, the isobutylene yield is ~70% (71.4% conversion and 95.6% selectivity) at 610 °C under the process conditions (15% i-C_4H_{10} in Ar). These results are close to the performance of industrial CrO_x/Al_2O_3 catalysts tested under similar conditions (Xing and Fridman, 2019).

The conversion for the Cr/Al_2O_3–0.7 catalyst synthesized by vacuum impregnation at 0.7 atm. is lower by 11–21 % mol. compared to the sample impregnated at 1.0 atm. The isobutylene selectivity for Cr/Al_2O_3–0.7 is also slightly lower by 0.2–1.3 %. Thus, a regular decreasing in conversion and selectivity is observed for a number of catalysts prepared by impregnation at 1.0, 0.85 and 0.7 atm.

To study the stability, the Cr/Al_2O_3-1.0 catalyst was tested during 25 catalytic cycles including oxidative regeneration and reductive activation between the dehydrogenation. It can be seen from Fig. 6b that relatively high stability is observed. The isobutane conversion is kept at 52–62% at 590 °C at a selectivity of 96–98%. This indicates the stability of active catalyst surface during the high-temperature oxidative-reductive treatments and relatively low amount of coke formed. The amount of coke was measured by TGA-DSC for Cr/Al_2O_3-1.0 catalysts after 3 catalytic cycles and cooling in inert atmosphere. The amount of coke was 1.26 %wt. after the cycle at 610 °C. This value is not high and the coke formation is an important process in the isobutane dehydrogenation in a fixed-bed reactor. The coke burning during the oxidative treatment leads to the catalyst bed overheating and this heat is used in the endothermic dehydrogenation process.

Thus, the analysis of results of catalytic and physical–chemical studies shows that for the catalysts prepared at 1.0, 0.85, and 0.7 atm, the following regularities are observed:

– a decreasing of specific surface area and pore volume due to partial blocking of pores by chromia,

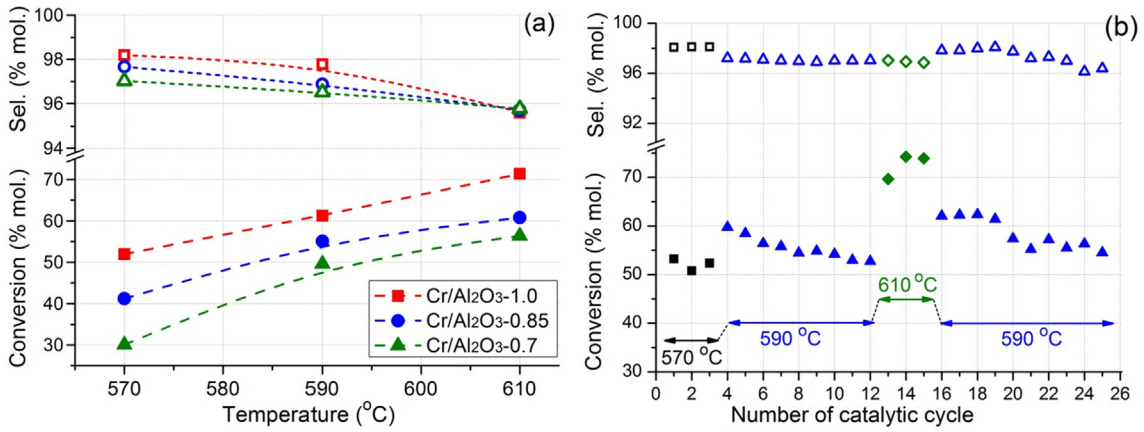

Fig. 6 Temperature dependences of isobutane conversion and isobutylene selectivity in the isobutane dehydrogenation over prepared catalysts (a), and the stability test for Cr/Al_2O_3-1.0 catalyst during 25 catalytic cycles (activation-dehydrogenation-regeneration).

– an increased amount of α-Cr_2O_3 with the growth of the particle size for this phase that is undesirable because the α-Cr_2O_3 phase is characterized by very low dehydrogenation activity,
– an increased temperature of Cr(VI) reduction indicating the Cr(VI) species agglomeration or enhanced chromia-support interaction that is also undesirable and leads to the decreased activity of chromia species,
– the decreased activity in a row Cr/Al_2O_3-1.0 > Cr/Al_2O_3-0.85 > Cr/Al_2O_3-0.7.

Thus, the preparation of CrO_x/Al_2O_3 catalysts is accompanied by many challenges: dissolving of alumina support in acidic impregnating solution, limited penetration of the impregnating solution inside the alumina support granules, etc. The decrease in the pressure during the impregnation of the granules of alumina support is a promising way to decrease the time of contact of support granules with the impregnating solution and enhance the penetration of impregnating solution inside the granules because of pressure change. However, the impregnation under vacuum leads to blocking of the support pores by chromia that is confirmed by the decreased S_{BET} and pore volume. A reduced catalytic activity may be a result of both reduction of active catalyst surface and increased amount of inactive α-Cr_2O_3 phase.

It is known that the dehydrogenation of light paraffins at 570–610 °C may be hindered by the internal diffusion of reagent to the active site and product elimination from the catalyst pores (Barghi et al., 2012,2014). A porous structure of the catalyst plays an important role in high-temperature processes (Lee and Kim, 2013). Wide mesopores and macropores provide isobutane diffusion towards active sites on the catalysts surface. Therewith the reaction products (isobutene and hydrogen) should be released from the active surface to prevent the hydrogenation reaction. Wide mesopores provide product transport from the catalyst granules. Blocking of the mesopores by chromia nanoparticles may be a reason for additional diffusion limitation and decreased activity of the catalysts prepared by vacuum impregnation. Besides, the Cr/Al_2O_3-1.0 catalyst prepared at atmospheric pressure is characterized by both relatively high surface area and the presence of macropores that was demonstrated by SEM and Hg intrusion porosimetry. Thus, the combination of macropores and relatively high surface area for this catalyst is favorable for relatively homogeneous distribution of the active component inside the alumina granules ("whole-egg" structure, Fig. 1b), high activity and stability in the isobutane dehydrogenation.

4. Conclusions

Thus, it was shown that the production of alumina-chromia catalysts is significantly limited by dissolution of the alumina support by impregnating solution containing chromic acid. Optimization of the impregnation conditions is required to synthesize highly active CrO_x/Al_2O_3 catalysts for dehydrogenation of light paraffins in a fixed-bed reactor. On the one hand, the time of impregnation should be minimized to prevent the alumina support dissolution by the impregnating solution containing chromic acid. On the other hand, the time and pressure of impregnation should provide penetration of the impregnating solution inside the alumina granules with a diameter of ~3 mm for the homogeneous distribution of active component and modifiers on the catalysts surface. The vacuum impregnation allowed us to introduce the impregnating solution rapidly, but it led to the decreased catalyst porosity as well as decreased activity in isobutane dehydrogenation. The role of macropores in the active component distribution during the impregnation and the role of macropores in minimization of diffusion limitations was demonstrated.

Declaration of Competing Interest

The authors declare that they have no known competing financial interests or personal relationships that could have appeared to influence the work reported in this paper.

Acknowledgment

This work was carried out within the framework of the state assignment of the Ministry of Science and Higher Education of the Russian Federation (project No. 0721-2020-0037). Author thanks Mrs. Elena Blokhina (Tomsk State University) for AES studies.

References

Barghi, B., Fattahi, M., Khorasheh, F., 2012. Kinetic modeling of propane dehydrogenation over an industrial catalyst in presence of oxygenated compounds. Reac. Kinet Mech. Cat. 107, 141–155. https://doi.org/10.1007/s11144-012-0455-z.

Barghi, B., Fattahi, M., Khorasheh, F., 2014. The modeling of kinetics and catalyst deactivation in propane dehydrogenation over Pt-Sn/γ-Al 2 O 3 in presence of water as an oxygenated additive. Petrol. Sci. Tech. 32 (10), 1139–1149. https://doi.org/10.1080/10916466.2011.631071.

Bekmukhamedov, G., Mukhamed'yarova, A., Egorova, S., Lamberov, A., 2016. Modification by SiO_2 of alumina support for light alkane dehydrogenation catalysts. Catalysts 6, 162. https://doi.org/10.3390/catal6100162.

Bugrova, T.A., Mamontov, G.V., 2018. The study of CrOx-containing catalysts supported on ZrO2, CeO2, and CexZr(1–x)O2 in isobutane dehydrogenation. Kinet Catal. 59 (2), 143–149. https://doi.org/10.1134/S0023158418020027.

Bugrova, T.A., Dutov, V.V., Svetlichnyi, V.A., Cortés Corberán, V., Mamontov, G.V., 2019. Oxidative dehydrogenation of ethane with CO_2 over CrO_x catalysts supported on Al_2O_3, ZrO_2, CeO_2 and $Ce_xZr_{1-x}O_2$. Catal. Today 333, 71–80. https://doi.org/10.1016/j.cattod.2018.04.047.

Bugrova, T.A., Mamontov, G.V., 2016. Dehydration of isobutane in fixed bed on the stable to carbon deposition chromia-alumina catalysts. Russ. J. Appl. Chem. 89, 1791–1796. https://doi.org/10.1134/S1070427216110094.

Bugrova, T., Tatarkina, A., Zhukov, I., Mamontov, G., 2016. Influence of wood flour additive on porous structure and strength properties of moulded alumina. Key Eng. Mater. 670, 139–143. https://doi.org/10.4028/www.scientific.net/KEM.670.139.

Busygin, V.M., Nesterov, O.V., Gilmanov, Kh.Kh., Romanov, V.G., Lamberov, A.A., Egorova, S.R., Bekmukhamedov, G.E., 2013. Catalyst of dehydration of C4-C5 paraffin hydrocarbons. RU Patent 2538960.

Cheng, Y., Zhang, F., Zhang, Y.i., Miao, C., Hua, W., Yue, Y., Gao, Z.i., 2015. Oxidative dehydrogenation of ethane with CO_2 over Cr supported on submicron ZSM-5 zeolite. Chin. J. Catal. 36, 1242–1248. https://doi.org/10.1016/S1872-2067(15)60893-2.

Darvishi, A., Davand, R., Khorasheh, F., Fattahi, M., 2016. Modeling-based optimization of fixed-bed industrial reactors for oxidative dehydrogenation of propane (ODHP). Chin. J. Chem. Eng. 24 (5), 612–622. https://doi.org/10.1016/j.cjche.2015.12.018.

Ertl, G., Knözinger, H., Schüth, F., Weitkamp, J., 2008. Handbook of Heterogeneous Catalysis, 8 Volume Set, 2nd ed., Wiley, Weinheim.

Fattahi, M., Khorasheh, F., Sahebdelfar, S., Tahriri, Z.F., Ganji, K., Saeedizad, M., 2011. The effect of oxygenate additives on the performance of Pt-Sn/γ-Al_2O_3 catalyst in propane dehydrogenation process. Scientia Iranica 18 (6), 1377–1383. https://doi.org/10.1016/j.scient.2011.08.015.

Fattahi, M., Kazemeini, M., Khorasheh, F., Darvishi, A., Rashidi, A. M., 2013. Fixed-bed multi-tubular reactors for oxidative dehydrogenation in ethylene process. Chem. Eng. Technol. 36 (10), 1691–1700. https://doi.org/10.1002/ceat.201300148.

Fridman, V., Urbancic, M.A., 2015. Dehydrogenation process with heat generating material. US Patent 20150259265.

Fridman, V.Z., Xing, R., Severance, M., 2016. Investigating the CrO_x/Al_2O_3 dehydrogenation catalyst model: I. identification and stability evaluation of the Cr species on the fresh and equilibrated catalysts. Appl. Catal., A. 523, 39–53. https://doi.org/10.1016/j.apcata.2016.05.008.

Fridman, V., 2012. Catalyst for dehydrogenation of hydrocarbons. US Patent 8101541

Gilmanov, Kh.Kh., Sakhabutdinov, A.G., Belanogov, I.A., Gusamov, R.R., Gilmullin, R.R., Sosnovskaya, L.B., 2015. Plant for dehydrogenation of paraffins or isoparaffins C3-C5 in chromia-alumina catalyst fluidized bed. RU Patent 2591159.

Kataev, A.N., Egorov, A.G., Egorova, S.R., Lamberov, A.A., 2015. Mathematical modeling of changes in the fractional composition of dehydrogenation catalysts in a fluidized-bed reactor. Catal. Ind. 7, 221–226. https://doi.org/10.1134/S2070050415030071.

Lee, J., Kim, D.H., 2013. Global approximations of unsteady state adsorption, diffusion, and reaction in a porous catalyst. AIChE J. 59, 2540–2548. https://doi.org/10.1002/aic.14014.

Li, B., Xu, Z., Chu, W., Luo, S., Jing, F., 2017. Ordered mesoporous Sn-SBA-15 as support for Pt catalyst with enhanced performance in propane dehydrogenation. Chin. J. Catal. 38, 726–735. https://doi.org/10.1016/S1872-2067(17)62805-5.

Li, Y., Zhang, Z., Wang, J., Ma, C., Yang, H., Hao, Z., 2015. Direct dehydrogenation of isobutane to isobutene over carbon catalysts. Chin. J. Catal. 36, 1214–1222. https://doi.org/10.1016/S1872-2067(15)60914-7.

Li, L., Zhu, W., Shi, L., Liu, Y., Liu, H., Ni, Y., Liu, S., Zhou, H., Liu, Z., 2016. The effect of ethanol on the performance of CrO_x/SiO_2 catalysts during propane dehydrogenation. Chin. J. Catal. 37, 359–366. https://doi.org/10.1016/S1872-2067(15)61042-7.

Long, L.-L., Lang, W.-Z., Liu, X., Hu, C.-L., Chu, L.-F., Guo, Y.-J., 2014. Improved catalytic stability of PtSnIn/xCa–Al catalysts for propane dehydrogenation to propylene. Chem. Eng. J. 257, 209–217. https://doi.org/10.1016/j.cej.2014.07.044.

Mamontov, G.V., Bugrova, T.A., Magaev, O.V., Musich, P.G., Zolotukhina, A.I., Merk, A.A., 2017. Dehydrogenation catalyst of light paraffin hydrocarbons and production method of unsaturated hydrocarbons with its use. RU Patent 2627664.

Nemykina, E.I., Pakhomov, N.A., Danilevich, V.V., Rogov, V.A., Zaikovskii, V.I., Larina, T.V., Molchanov, V.V., 2010. Effect of chromium content on the properties of a microspherical alumina-chromium catalyst for isobutane dehydrogenation prepared with the use of a centrifugal thermal activation product of gibbsite. Kinet. Catal. 51, 898–906. https://doi.org/10.1134/S0023158410060169.

Neri, G., Pistone, A., De Rossi, S., Rombi, E., Milone, C., Galvagno, S., 2004. Ca-doped chromium oxide catalysts supported on alumina for the oxidative dehydrogenation of isobutene. Appl. Catal., A. 260, 75–86. https://doi.org/10.1016/j.apcata.2003.10.002.

Otroshchenko, T., Sokolov, S., Stoyanova, M., Kondratenko, V.A., Rodemerck, U., Linke, D., Kondratenko, E.V., 2015. ZrO 2 -based alternatives to conventional propane dehydrogenation catalysts: active sites, design, and performance. Angew. Chem. Int. Ed. 54, 15880–15883. https://doi.org/10.1002/anie.201508731.

Otroshchenko, T., Radnik, J., Schneider, M., Rodemerck, U., Linke, D., Kondratenko, E.V., 2016. Bulk binary ZrO 2 -based oxides as highly active alternative-type catalysts for non-oxidative isobutane dehydrogenation. Chem. Commun. 52, 8164–8167. https://doi.org/10.1039/C6CC02813F.

Rodemerck, U., Sokolov, S., Stoyanova, M., Bentrup, U., Linke, D., Kondratenko, E.V., 2016. Influence of support and kind of VO_x species on isobutene selectivity and coke deposition in non-oxidative dehydrogenation of isobutene. J. Catal. 338, 174–183. https://doi.org/10.1016/j.jcat.2016.03.003.

Rodemerck, U., Kondratenko, E.V., Otroshchenko, T., Linke, D., 2016. Unexpectedly high activity of bare alumina for non-oxidative isobutane dehydrogenation. Chem. Commun. 52, 12222–12225. https://doi.org/10.1039/C6CC06442F.

Rodemerck, U., Stoyanova, M., Kondratenko, E.V., Linke, D., 2017. Influence of the kind of VO_x structures in VO_x/MCM-41 on activity, selectivity and stability in dehydrogenation of propane and isobutene. J. Catal. 352, 256–263. https://doi.org/10.1016/j.jcat.2017.05.022.

Rombi, E., Cutrufello, M.G., Solinas, V., De Rossi, S., Ferraris, G., Pistone, A., 2003. Effects of potassium addition on the acidity and reducibility of chromia/alumina dehydrogenation catalysts. Appl.

Catal A. 251, 255–266. https://doi.org/10.1016/S0926-860X(03)00308-9.

Ruettinger, W., Jacubinas, R., 2016. Chromia alumina catalysts for alkane dehydrogenation. US Patent 9254476.

Ruettinger, W., Breen, M.J., Jacubinas, R., Alerasool, S., 2010. Alkane dehydrogenation catalysts. US Patent 20100312035.

Salaeva, A.A., Salaev, M.A., Vodyankina, O.V., Mamontov, G.V., 2019. Synergistic effect of Cu and Zn modifiers on the activity of CrO_x/Al_2O_3 catalysts in isobutane dehydrogenation. Appl. Catal. A: Gen. 581, 82–90. https://doi.org/10.1016/j.apcata.2019.05.018.

Salaeva, A.A., Salaev, M.A., Mamontov, G.V., 2020. Effect of Cu modifier on the performance of CrO_x/Al_2O_3 catalysts for isobutane dehydrogenation. Chem. Eng. Sci. 215. https://doi.org/10.1016/j.ces.2019.115462.

Sattler, J.J.H.B., Ruiz-Martinez, J., Santillan-Jimenez, E., Weckhuysen, B.M., 2014. Catalytic dehydrogenation of light alkanes on metals and metal oxides. Chem. Rev. 114, 10613–10653. https://doi.org/10.1021/cr5002436.

Shee, D., Sayari, A., 2010. Light alkane dehydrogenation over mesoporous Cr_2O_3/Al_2O_3 catalysts. Appl. Catal. A 389, 155–164. https://doi.org/10.1016/j.apcata.2010.09.013.

Słoczyński, J., Grzybowska, B., Kozłowska, A., Samson, K., Grabowski, R., Kotarba, A., Hermanowska, M., 2011. Effect of potassium on physicochemical properties of CrO_x/Al_2O_3 and CrO_x/TiO_2 catalysts for oxidative dehydrogenation of isobutane: The role of oxygen chemisorption. Catal. Today 169, 29–35. https://doi.org/10.1016/j.cattod.2010.10.096.

Spanos, N., Slavov, S., Kordulis, Ch., Lycourghiotis, A., 1994. Mechanism of deposition of the CrO42-, HCrO4-, and Cr2O72-ions on the gamma-alumina surface. Langmuir. 10, 3134-3147. https://doi.org/10.1021/la00021a042

Tian, Y.-P., Bai, P., Liu, S.-M., Liu, X.-M., Yan, Z.-F., 2016. VO_x–K_2O/γ-Al_2O_3 catalyst for nonoxidative dehydrogenation of isobutene. Fuel Process. Technol. 151, 31–39. https://doi.org/10.1016/j.fuproc.2016.05.024.

Xing R., Fridman V. 2019. Dehydrogenation catalysts. Patent US 2019/0126242 A1.

Xu, Y., Sang, H., Wang, K., Wang, X., 2014. Catalytic dehydrogenation of isobutane in the presence of hydrogen over Cs-modified Ni 2 P supported on active carbon. Appl. Surf. Sci. 316, 163–170. https://doi.org/10.1016/j.apsusc.2014.07.119.

Xu, L., Wang, Z., Song, H., Chou, L., 2013. Catalytic dehydrogenation of isobutane over ordered mesoporous Cr_2O_3–Al_2O_3 composite oxides. Catal. Commun. 35, 76–81. https://doi.org/10.1016/j.catcom.2013.02.011.

Zhao, H., Song, H., Xu, L., Chou, L., 2013. Isobutane dehydrogenation over the mesoporous Cr_2O_3/Al_2O_3 catalysts synthesized from a metal-organic framework MIL-101. Appl. Catal. A 456, 188–196. https://doi.org/10.1016/j.apcata.2013.02.018.

Zhou, H., Gong, J., Xu, B., Deng, S., Ding, Y., Yu, L., Fan, Y., 2017. An efficient catalyst for propane dehydrogenation. Chin. J. Catal. 38, 529–536. https://doi.org/10.1016/S1872-2067(17)62750-5.

Zykova, A., Livanova, A., Kosova, N., Godymchuk, A., Mamontov, G., 2015. Aluminium oxide-hydroxides obtained by hydrothermal synthesis: influence of thermal treatment on phase composition and textural characteristics. IOP Conf. Ser.: Mater. Sci. Eng. 98. https://doi.org/10.1088/1757-899X/98/1/012032.